Newly Identified Effects of Injector Nozzle Fouling in Diesel Engines

Burke, R.D.[1*], Madamedon, M.[1], Williams, R.[2]

1. Institute for Advanced Automotive Propulsion Systems (IAAPS), University of Bath, Bath, BA2 7AY
2. Shell Global Solutions UK,

* Corresponding Author: T: +441225383481, e: r.d.burke@bath.ac.uk

Keywords: Diesel Engine, Injector fouling, thermal efficiency, NOx emissions

1 Abstract

This paper describes newly identified effects of fouled injectors in diesel engines. As well as restricting and disrupting fuel flow into the combustion chamber, injector fouling has wider impacts on the engine, and these form the focus of this work. Injector fouling was induced synthetically through the addition of zinc to two types of Diesel fuel on a 2.2L engine. A new degree of fouling metric was presented that allows for a consistent comparison of fouling at full and part load. The investigation has identified impacts on air and fuel pumping losses and on combustion phasing that deteriorate brake thermal efficiency by up to 3%. The effects were also seen during a transient cycle representative of on-road conditions (WLTC). This is significant because the effects of injector fouling are typically only studied at high loads and under steady state conditions. The WLTC results also demonstrated an increase in NOx (9%-18%) and CO_2 (up to 1%) emissions as a result of nozzle deposits. The magnitudes of fouling effects were found to vary both with base fuel type and with test condition. A premium dose rate of performance fuel additive was effective at cleaning up the deposits and restoring normal engine performance.

2 Introduction

The fouling of injectors in internal combustion engines is a widespread problem, particularly in automotive applications, that can impair power, fuel economy and emissions. The impact of fouled injectors is not always detectable in motor compliance tests (such as UK MOT test) due to the subtle way in which these effects sometimes manifest themselves. Therefore, prevention remains the most effective method to avoid the impacts from injector fouling by using cleaning additives in the fuels. However the overall effectiveness of this approach depends on customers choosing to purchase the quality fuels which contain these additives. This paper describes newly identified effects of fouled injectors which apply in addition to the conventional metrics of power and fuel economy and provide a new understanding of the effects of injector fouling. In section 2, a review of previous work is presented. Section 3 then presents the experimental approach and modelling methodology. Section

4 will present the results and basic analysis before section 5 provides a wider interpretation of these results and their implications. Section 6 draws the main conclusions from the work.

3 Background

Diesel injector deposits can occur in different parts of the injector. In the nozzle, the deposits can occur when liquid fuel evaporates under high temperature, leaving sticky residues on which deposits can accumulate [1, 2]. Traces of metallic components within the fuel (Na, Zn, Cu and Ca) can encourage fuel oxidation and form ash-containing deposits which are difficult to remove through the normal thermal cycling of the engine [3-5]. The processes are the result of opposing chemical mechanisms that occur at both lower and higher temperatures [6]. Whilst historically injector fouling was initially focussed on Diesel engines, there is increasing interest in fouling in gasoline direct injection systems [7-12]. As well as deposits forming in the nozzle that restrict and disrupt fuel flow, results such as those published by Magno et al. [13] suggest that deposits may also adversely affect injector control as they observed increases in pilot fuelling quantities suggesting a slower response of the control valves or needle. These Internal Diesel Injector Deposits (IDIDs) form inside the injector and are outside the scope of the current study.

There are a number of factors that influence diesel injector nozzle deposit formation: geometric design of injector, tip temperature and fuel quality. Fuel additives are the most effective way to supress deposit formation [6]. Evidence has shown that injector fouling is a reversible process and that with the appropriate additives deposit removal can be an order of magnitude faster than deposit formation [14, 15].

Lab based experiments are common for evaluating the formation of deposits and the ability of fuel additives to remove and/or suppress the formation of deposits. In the laboratory, the dosing of traces of zinc compounds (up to 3ppm Zn) [15] is most commonly used to induce fouling as this is an element with one of the strongest fouling tendencies [14, 16] and is found as a contaminant in vehicle fuel systems [17]. The lab-based studies seek to accelerate the formation of deposits by creating conditions which are more favourable to their formation. For the past 10 years, a standard fouling cycle has been used as proposed by the Coordinating European Council (CEC F98-08 test, more commonly known as DW10B test). During the test development, some questions were raised as to the relevance of the cycle for in-service operation of light duty Diesel engines [18], however it is now commonly used as a standard for evaluating fuels and additives.

There is a body of research which looks at the direct measurement of the level of fouling which involves direct inspection of the injector. SEM (Scanning Electron Microscopy) is most common

but other techniques are used [19, 20]. The secondary effect of fouling is a reduction in fuel flow rate through the injector and this is most commonly used in laboratory experiments to quantify fouling either as a direct reduction in flow [11, 12, 21-24] or the reduction in engine torque or power resulting from the reduced flow. The level of power drop observed for a fouled injector compared to a clean injector depends on the engine and the fuel used, however over a typical CEC F98-08 test cycle, the reported power losses with 1-3 ppm concentration of zinc in the fuel range from 5% to 12% [5, 15, 18, 25-30].

The tertiary effects of injector fouling are much less studied. A number of authors have looked at the impact of fouling on engine emissions, with a particular focus on particulates and hydrocarbons [9, 19, 31]. D'Ambrosio and Ferrari [24] demonstrate that the NOx/Soot EGR trade-off is worsened for fouled injectors. These influences seem to be caused by the disruption of the flow pattern which affects the shape and penetration of the spray into the combustion chamber, however there is no definitive description of how deposits affect the flow [10, 32, 33]. Only a few studies report fuel consumption changes which are typically in the order of 1% [1, 13, 26, 34]. There is currently a lack of published information quantifying any further tertiary effects of injector fouling or measuring the magnitude of these effects over typical in-service operating conditions. As such, the aim of this work is to identify new measurements of engine behaviour resulting from injector fouling. These effects will be shown to be reversible during injector clean-up and quantified for a range of engine operating conditions.

4 Methodology

An adapted version of the CEC F98-08 injector fouling test was used to induce deposit formation on a 2.2L EURO 5 specification Diesel. Fouling was performed over a 32h test period by dosing 6ppm of zinc neodecanoate (6ppm Zn) into the fuel. The subsequent 24h clean-up process was completed by adding a cleaning additive to the zinc dosed fuel. The complete fouling – clean-up cycle was conducted sequentially with two fuels and the same injector set, firstly a B7 diesel (7% FAME) which was a mixture of German market fuels, and secondly a CEC B0 reference Diesel fuel, RF79-07, which is specified for the CEC F98-08 test. Both fuels complied with the EN590 specification. Two WLTC test cycles were conducted each time the injectors were in clean and fouled state, one following an overnight soak at 23°C and the second under hot start conditions. An overview of the experiment is given in Table 5. Throughout the experimental campaign, a substantial array of engine instrumentation was used to measure factors indicative of changes to engine efficiency. Where necessary, data analysis was supported by the use of a 1D wave action model to isolate specific fouling induced effects.

4.1 Experimental Setup

4.1.1 Engine and test rig

The engine used in this study is a 2.2L EURO 5 specification Diesel engine with common rail fuel injection system that is fitted to a range of light-duty diesel passenger and commercial vehicles. The engine specifications are given in table 1. The engine was installed on a 215kW transient dynamometer in a test cell with dedicated HVAC (Heating, Ventilation and Air Conditioning) system to ensure consistent engine soaking temperature. The test fuel was supplied to the engine from a drum via a lift pump and production-standard filter to the test cell gravimetric fuel balance. Fuel was then gravity fed to the test cell lift pump before flowing through the main temperature conditioning system which controlled fuel temperature to 50°C. Fuel consumption was determined primarily by a second flow meter (Kistler DFL3) as shown in Figure 1b below.

Table 1: Engine characteristics

Displacement	2.2L
Emissions Specification	EURO 5
Aftertreatment	DOC + DPF*
Design	4 cylinders in line, variable geometry turbocharger with High Pressure EGR
Combustion chamber	Four valves, bowl in piston, direct injection
Max. Power	115kW
Max. Torque	~400Nm
Injection system	Common rail with piezo actuated servo control Hole-type Injector nozzle with 8 holes Max injection pressure 1800bar

* Only the DOC was fitted for the experiments conducted in this paper

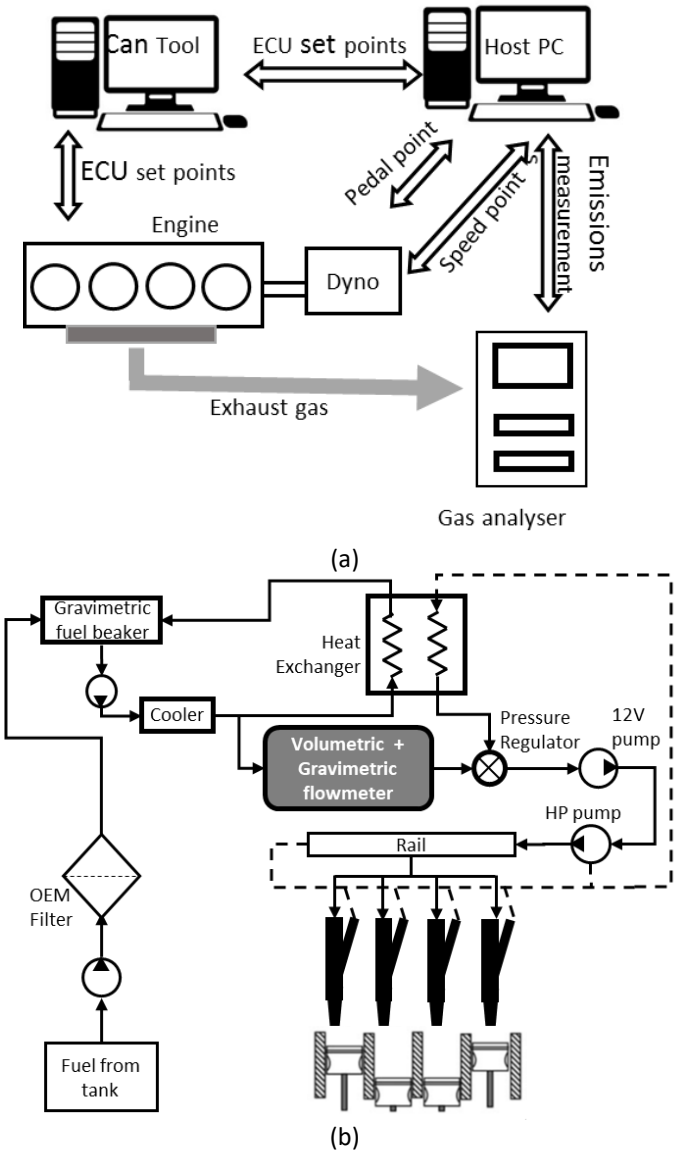

Figure 1: Test cell layout showing (a) engine test bed and (b) fuel supply system

4.1.2 Instrumentation

The test facility is instrumented with pressure, temperature, mass flow and other relevant sensors. The location of the most important of these sensors is provided in figure 1 and the details of the instruments used detailed in table 2. Data from the sensors were sampled either at 10Hz using the Sierra CP Cadet host system, directly from the engine control unit using Accurate Technologies ATi Vision or crank angle resolved using a Dewetron 800 series high frequency logging system. The crank angle resolved data was used to calculate a series of combustion and indication parameters as follows:

- Indicated and Pumping mean effective pressure (IMEP and PMEP)

$$IMEP = \oint PdV \qquad 1$$

$$PMEP = \int_{EVO}^{IVC} PdV \quad \mathbf{2}$$

123

124 - Peak cylinder pressure
125 - Angle of peak cylinder pressure
126 - 10%, 50% and 90% burn angles

127 The heat release parameters are calculated by applying the first law of thermodynamics to
128 the combustion chamber such that the rate of heat release from combustion is the sum of the change
129 in internal energy, heat and work transfers and enthalpy transfers through the valves and blow-by
130 gases. The enthalpy flows can be ignored if the calculation is applied when intake and exhaust valves
131 are closed and in this paper blow-by is ignored. Ignoring blow-by has been shown to cause a maximum
132 error of 1.4% in heat release calculation and the largest errors are at low speeds and loads [35].

$$dQ_c = dU - dQ_{HT} - dW \quad \mathbf{3}$$

133

134 The change in internal energy can be calculated from equation 4 where the in-cylinder
135 temperature is calculated using the measured pressure and the perfect gas law (equation 5). The heat
136 losses at the cylinder wall were estimated using the Hohenberg correlation [36]

$$dU = m_{cy} c_{p,cy} dT_{cy} \quad \mathbf{4}$$

137

$$T_{cy} = \frac{p_{cy} V_{cy}}{m_{cy} R} \quad \mathbf{5}$$

138

139 The work term is estimated from measured cylinder pressure (equation 6).

$$dW = p_{cy} dV_{cy} \quad \mathbf{6}$$

140

141 Details of the heat release calculation can be found in [35]. For this work, the in-cylinder mass
142 was estimated by assuming that conditions in the cylinder are similar to those in the intake manifold
143 at Intake valve closing. The measured pressure signal was referenced using the 2-point method with
144 a fixed polytropic index assumed to be 1.3 [35].

145

Table 2: Details of key sensors used in this work

Type	Measurements	Instrument	Range	Accuracy
Air Mass Flow	Engine intake air	ABB Sensyflow	0-800kg/h	+/-1%
Temperature	Gas temperatures in air path	k-type thermocouple	0-1200K	+/-2.2°C
Temperature	Oil and Coolant	PRT	0-260°C	+/-0.3°C
Pressure	Fluid pressures in air path and oil circuit	Piezo-resistive pressure transducers	0-5bar	+/-0.015bar
Fuel flow	Engine fuel mass flow	Emerson Micro Motion ELITE Coriolis Flow meter	0-35kg/h	+/-0.1%
Fuel flow	Engine fuel volumetric flow	Kistler DFL3x-5bar	0.5-50l/h	+/-0.5%
Emissions volumetric concentrations	Feed gas gaseous concentrations of CO, CO_2, NOx and HC	Horiba MEXA 7000	CO_2: 0-20% CO: 0-5000ppm NOx: 0-10000ppm HC: 0-20000ppm	Not specified
In cylinder pressure	Combustion pressure	Kistler Type 6056A	0-250bar	+/-2%
Engine torque	Engine brake torque	HBM analogue torque sensor	-500-500Nm	0.05%
Injector current	Injector pulse signal	Kistler M705A current clamp	0-30A	Response time: 3us

4.2 Test methods

4.2.1 Duty cycles

A modified version of the CEC F98-08 cycle was used on this engine, modified to avoid problems encountered with engine derating at peak power conditions. This derating occurred due to hardware protection algorithms (such as turbocharger or catalyst temperature protection) occurring within the engine control strategy which could not be suppressed in the dynamometer configuration. The modified CEC cycle avoided the derating by limiting the engine speed range to 2000rpm. The resulting 12-point duty cycle points are listed in table 3 and compared to the standard CEC F98-08 cycle. The CEC modified cycles were run in batches of up to 4 tests with an engine restart every 3-4 cycles and an overnight soak every 6-8 cycles. A 20minute warm-up at 1500rpm/100Nm was conducted prior to the first CEC cycle following the overnight soak.

Table 3: Operating points for the modified CEC test used in this work compared with the standard CEC F98-08 cycle

Stage	Duration (min)	Load (%)	Engine Speed (r/min) ± 20		Torque (Nm) ± 5	
			CEC F98-08	Modified	CEC F98-08	Modified
1	2	(20)	1750	1750	70	70
2	7	(60)	3000	**2000**	200	225
3	2	(20)	1750	1750	70	70
4	7	(80)	3500	**2000**	240	300
5	2	(20)	1750	1750	70	70
6	10	100	4000	**2000**	240	370
7	2	(10)	1250	1250	30	30
8	7	100	3000	**2000**	340	370
9	2	(10)	1250	1250	30	30
10	10	100	2000	2000	370	370
11	2	(10)	1250	1250	30	30
12	7	100	4000	**2000**	240	370

The engine was also tested over a WLTC transient driving cycle before and after each fouling and clean up stage, by emulating the vehicle speed and load and driver gear shifting logic. The engine speed and torque setpoints for the WLTC cycle were defined for a typical light duty truck application for this engine. Details of the vehicle emulation are provided in the appendix.

4.2.2 Fuel types and blending and fuel test programme

Two base fuels were used sequentially for a 32h dirty-up and subsequent 24h clean-up cycles:

- B7 Diesel/biodiesel comprising a mixture of German market fuels
- RF79-07 reference fuel specified for the CEC F98-08 industry standard injector deposit rating (DW10B) test

Both fuels conformed to the EN590 specification.

Zinc neodecanoate, as specified in the CEC DW10B industry standard test (F98-08) was used as a contaminant to induce fouling. The zinc was dissolved into Hamsol 150 solvent and dosed into the fuel and in each case the fuel blending was conducted on the same day as it was used for testing. To achieve sufficiently high levels of fouling in acceptable test durations, zinc was dosed with a target concentration of 6ppm, which is above the 1-3ppm levels typically used in industry standard tests. The achieved levels of zinc concentration were measured using Inductively Coupled Plasma Spectroscopy: these results were quite variable but 90% of samples showed a concentration achieved in the fuel of 3ppm or greater and all samples were greater than 1ppm. The project timeline and resources did not

allow for the fuel zinc level variability to be solved or indeed for it to be conclusively attributed to the fuel blending or zinc measurement method. Given that there was no intent to compare between a range of tests, these limitations were deemed acceptable given that sufficient zinc was included to provoke a fouling signal.

The fuels test programme is summarised in table 4. For both Fouling and clean up, zinc was added to the fuel. During clean up a premium dose rate of a performance additive package was also included. All the WLTC cycles were conducted using zinc- and additive-free reference fuel. Fuel was fully flushed through the engine system at each fuel change.

Table 4: Fuel testing programme

Test phase	Fuel	Test cycles
Clean up 0	B7 + Additive	32h modified CEC cycle
Clean WLTC 1	RF79-07	Hot/cold WLTC test
Fouling 1	B7+6ppm Zn Neo	32h modified CEC cycle
Dirty WLTC 1	RF79-07	Hot/cold WLTC test
Clean up 1	B7+6ppm Zn Neo +Additive	24h modified CEC cycle
Clean WLTC 2	RF79-07	Hot/cold WLTC test
Fouling 2	RF79+6ppm Zn Neo	32h modified CEC cycle
Dirty WLTC 2	RF79-07	Hot/cold WLTC test
Clean up 2	RF79+6ppm Zn Neo +Additive	24h modified CEC cycle
Clean WLTC 3	RF79-07	Hot/cold WLTC test

4.3 Engine model

A 1D wave action model of the engine was used to investigate further and isolate some of the measured parameters within the engine. The model includes a full 1D wave dynamic model of the external air path including the inlet and exhaust manifolds, turbocharger, intercooler and EGR hardware. Engine breathing has been parameterised using empirical data. Of key relevance to this work is the combustion model. The model discretizes the content of a cylinder into three thermodynamic zones; the main unburned zone, the spray unburned zone and the spray burned zone, with each zone having their own composition and temperature. The main unburned zone contains all cylinder mass at the close of intake valve, the spray unburned zone contains injected fuel and entrained gas and the spray burned zone contains combustion product. The model includes some sub-models which simulate relevant physical processes taking place during injection and combustion events.

The heat release model is a mixing-controlled combustion model including ignition delay, and premixed and diffusion combustion models. Details of this model are beyond the scope of this work but are detailed by Dowell et al [39]. The parameters of this model have been tuned empirically using

steady state data from across the engine operating map. The model was used to simulate the effect of fouled injectors on the combustion and heat release process. In particular, fouled injectors reduce fuel flow and therefore to maintain the same mass of injected fuel when fouled the fuel must be injected over a longer period of time and/or at a higher pressure. If the fuel is injected over a longer period, combustion can be elongated. As such, the fouled injectors were simulated by reducing the rate of diffusion combustion. The rate was reduced by a magnitude sufficient to change the centre of combustion to that observed experimentally on the test engine.

5 Results and discussion

5.1 Level of fouling achieved

Injector fouling is usually quantified by a reduction in fuel flow or in engine peak power. However, the engine operating point can mask some of the fouling effects. At part load conditions with constant torque output, as defined in the CEC F98-08 test cycle, injector fouling does not prohibit the engine from reaching the target torque, however in order to reach this level of torque the injector pulse width must be increased. In practice this occurs because the test cell control system increases actuation on the accelerator pedal, which in turn makes the engine operate at a higher target load point. The higher fuelling demand is balanced by the restricted fuel flow in the fouled injector and the resultant engine output torque is the same as for a clean injector with lower target load point and shorter injector pulse width. So, during part load engine operating conditions, increase in pedal position can be an indication of fouled injectors as shown in figure 2a.

In contrast, at full load the accelerator pedal position is maintained at 100% and injector fouling and resultant drop in fuel flow rate manifests itself as a drop in engine power (figure 2b). This is consistent with previous studies. For this work, the drop in engine power over the 32h fouling was 4% and 8% for B7 and reference fuels respectfully. This is less than some values typically seen in the CEC F98-08 test, however this is a different engine and fuel injection system to the DW10B engine used within that test which is likely to be a major factor in these differences. Pertinently, the DW10B configured for the CEC F98-08 test is fitted with injector nozzles that are specially machined to reduce flow cavitation and thus increase sensitivity to injector deposit formation.

The results in figure 2 clearly show evidence of injector fouling during the 32h of fouling tests followed by a reversal in the trends during clean up. This showed that the fouling and clean-up action are reversible and repeatable within this engine setup and testing procedure.

During these tests it was observed that the fuel injected quantity commanded by the ECU (‘fuelling demand’) sometimes varied in response to varying lambda values. This then reduced the

accuracy of using simply torque at full load or pedal position at part load as the primary indices of injector fouling level.

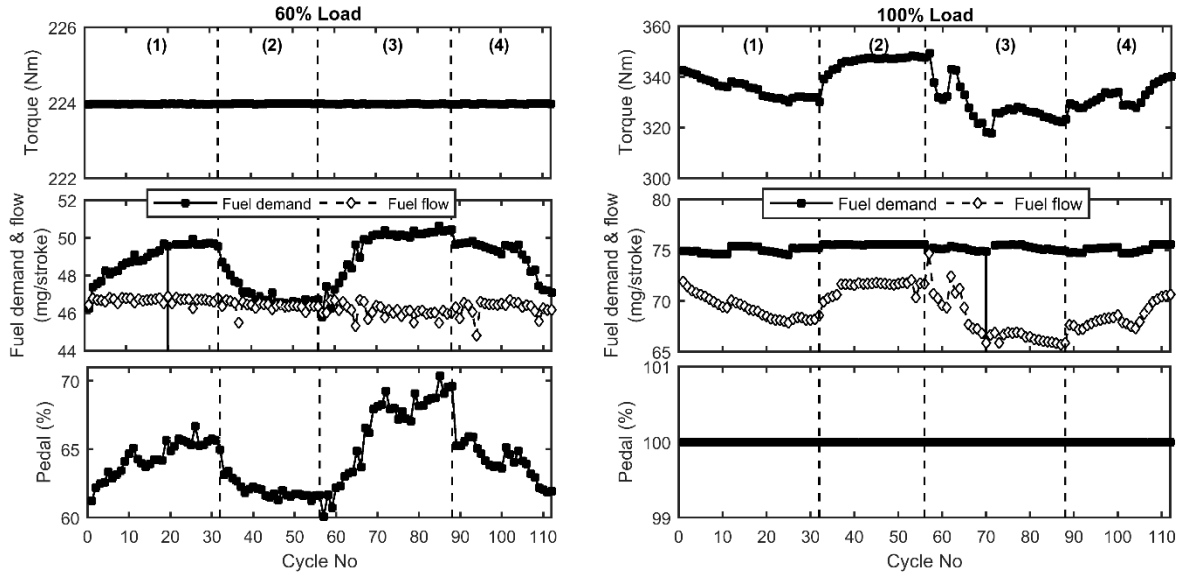

Figure 2: Change in output torque and accelerator pedal position during fouling/clean up cycles at (a) part load and (b) full load

To be able to compare the level of fouling at both part load and full load, a new metric is proposed which is the ratio of the engine's output torque to its fuel demand. The engine fuel demand is a variable used within the engine control unit which can be interpreted as a desired fuelling quantity. The controller uses it to calculate the required injection pulse width and is therefore a useful indicator of how much fuel the engine controller *intended* to inject. The output torque is a good measure of how much fuel was burnt within the engine and therefore can be used as a metric of how much fuel was injected. The metric is also normalised to allow for a direct comparison at different operating points (equation 7)

$$Fouling\ Rate = \frac{\tau_{Brake}}{\dot{m}_{f,DEMAND}} \qquad 7$$

As deposits form on the injector and restrict fuel flow, the amount of fuel injected will reduce for the same fuelling demand – this will hold true for both a full and part load allowing for a single metric that can be compared at different operating points. The metric is illustrated in figure 3. The benefits of the metric are two-fold:

1. This metric provides a common trend across both full and part load points and can therefore provide a comparison of the degree of fouling from an engine performance perspective across the engine operating map.
2. This engine exhibited changes in fuelling demand at full load despite the pedal remaining at 100%. This could be related to aspects in the control strategy around hardware protection. Whatever the cause, these changes in fuelling demand will affect the engine torque output which will undermine the use of torque as a measure of the degree of fouling. The proposed metric normalises for this.

It can clearly be seen that whilst for the B7 fuel the fouling is completely reversible during the 24h clean-up phase with the fuel additive, a complete reversal is not achieved during the initial 16h clean-up with the reference fuel. A continued reversal of the factors was only seen once the zinc was removed from the fuel before a further 8h of running.

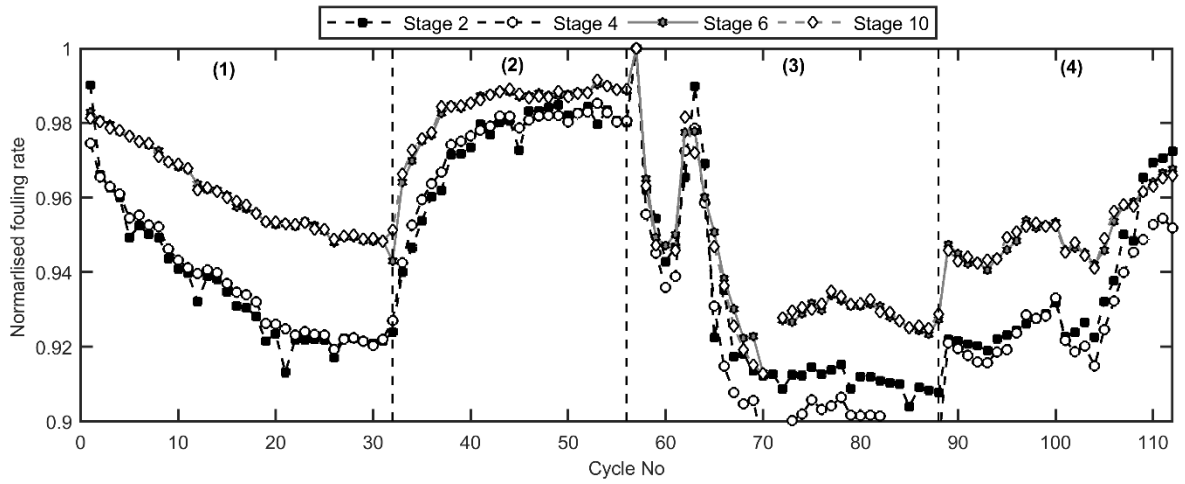

(1) B7 Dirty-up (2) B7 Clean up (3) RF79-07 Dirty-up (4) RF79-07 Clean-up

Figure 3: New fouling metric defined as the ratio of fuelling demand to output torque allows quantification of degree of fouling both at full and part load

5.2 CEC Results

5.2.1 Full load results

It was shown in figure 2 that at full load, the mass of fuel injected into the cylinder is reduced with fouled injectors. There are however further implications for the engine performance that need to be accounted for.

The reduced fuelling quantity will also result in lower exhaust gas temperature and reduced enthalpy available to the turbocharger. Figure 4 clearly shows a drop in exhaust temperature over the 32h of fouling of 25°C and 35°C for B7 and Reference fuel respectively. As the engine pedal position

remains at 100%, the engine controller still operates as if it were injecting the maximum fuel quantity. This means the other engine setpoints remain unchanged. One example is the target boost pressure - figure 4 shows that the intake manifold pressure remains constant throughout the fouling-clean-up cycle at around 150kPa. To maintain the constant intake manifold pressure with reduced exhaust enthalpy (as a result of the lower exhaust temperature), the engine is required to close the guide vanes of the variable geometry turbocharger by 2-3%. This in turn increases the engine back pressure (by 7-15kPa). Overall this results in an increase in pumping losses, quantified through an increase in PMEP from 0.1bar to 0.18-0.2bar.

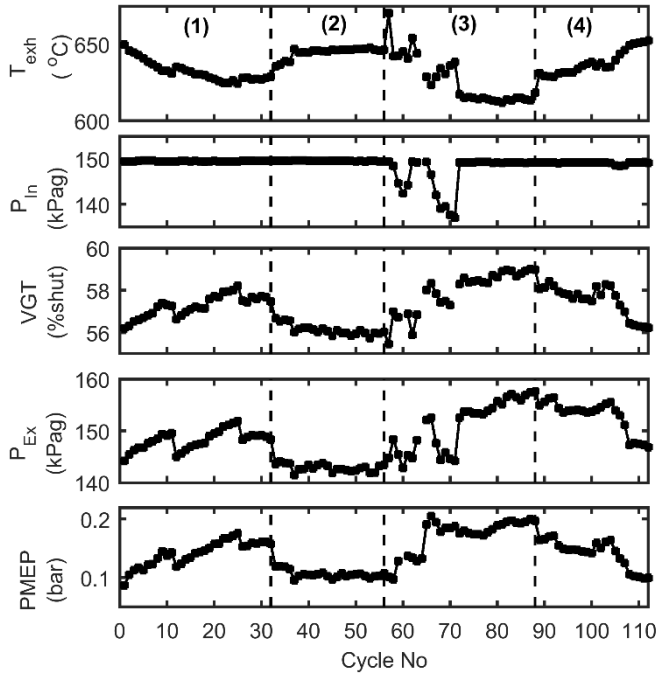

Figure 4: Changes in pumping losses at full load as a result of reduced exhaust enthalpy due to injector fouling

5.2.2 80% Part Load Results

At the 80% load/2000rpm condition (stage 4 of the modified CEC test), the pedal position is gradually increased by the test cell host system as the degree of fouling increases to maintain the same output torque despite the reduction in injector flow. The change in accelerator pedal position increases the duration of the main injection by increasing the injector pulse width as compared for the clean and fouled condition in figure 5. The injector signal in figure 5 is characteristic of piezo injectors. In contrast to solenoid injectors which have a peak and hold current form, piezo injectors exhibit a current pulse as the injector opens and an inverse current pulse as the injector closes (in this

case a negative pulse for opening and a positive pulse for closing). Consequently figure 5 shows a pilot injection at about -25°CA with injector closing occurring almost immediately after injector opening and the main injection starting at -5°CA and ending at 10°CA for clean injectors and 12°CA for fouled injectors.

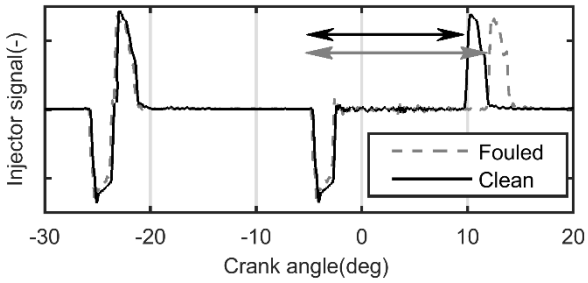

Figure 5: Injector pulse width for B7 fuel at 80% load for clean and fouled conditions

The change in pulse width is gradual as shown in figure 6b. This is the only major impact at this operating condition from the increased pedal position as it can be seen that changes in main injection timing (figure 6c) and fuel injection pressure (figure 6d) are small.

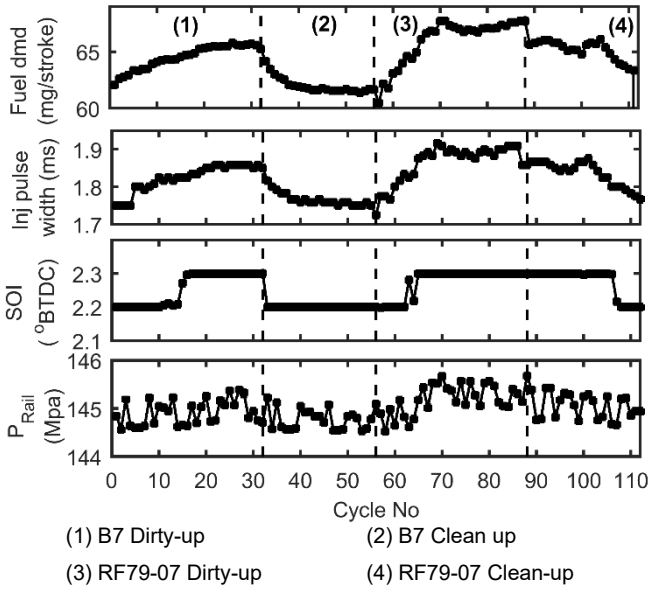

Figure 6: Change in fuel demand, injector pulse width, main injection timing and fuel pressure in the rail over the fouling/clean up cycles.

The increased injector pulse width increases the duration of injection. Given that very little change occurs in the start of injection, the end of injection must occur later (as seen in figure 5), this means it would be expected that the combustion will occur over a longer period. This is confirmed by a later heat release in the fouled condition and the measured change in centre of combustion (AI50) as the level of fouling increases shown in figure 7. AI50 is shown to be delayed by around 0.8°CA for B7 and 1.3°CA for Ref fuel. The shift in AI50 is seen to revert during the clean-up cycle.

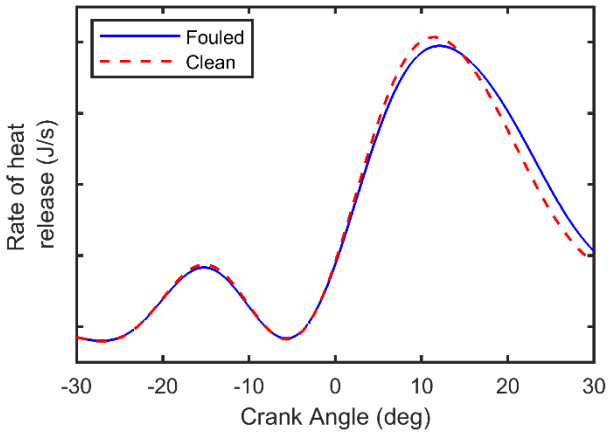

(a)

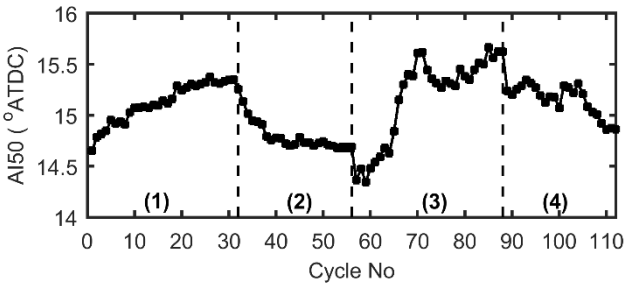

(b)

(1) B7 Dirty-up (2) B7 Clean up

(3) RF79-07 Dirty-up (4) RF79-07 Clean-up

Figure 7: (a) evolution of heat release for clean and fouled conditions with B7 and (b) change in 50% burn angle (AI50) through fouling and clean up cycles at 80% load/2000rpm

The delayed combustion could be responsible for lower thermal efficiency of the diesel cycle. To investigate this further and isolate the effect of longer combustion duration, a series of simulations were conducted in the 1D engine simulation. The change in combustion duration was implemented by changing the diffusion combustion rate multiplier of the predictive direct injection diesel multi-pulse combustion model. Five cases were simulated for each fuel, each replicating different stages of the fouling cycles measured in the engine tests. Other engine boundary conditions were taken directly from measurements with only AI50 being varied (through a change in diffusion combustion rate as detailed in section 4.3). The simulated values of AI50 are reported in table 5 along with key metrics quantifying the thermodynamic cycle.

340 **Table 5: Simulation parameters and efficiency indicators due to a change in AI50 at 80%**
341 **load**

Fuel	AI50 (°CA)	Change in IMEP (bar)	Change in Brake Torque (Nm)	Change in thermal efficiency (%)
B7	14.25	0	0	0
	14.63	-0.08	-1.41	-0.15
	14.82	-0.17	-2.9	-0.3
	15.02	-0.26	-4.48	-0.47
	15.16	**-0.34**	**-5.81**	**-0.61**
Reference Fuel	14.25	0	0	0
	14.63	-0.08	-1.32	-0.14
	14.89	-0.16	-2.71	-0.29
	15.23	-0.36	-6.14	-0.65
	15.58	**-0.59**	**-9.95**	**-1.05**

342

343 *5.2.3 60% part load results*

344 Similar to the 80%/2000rpm case, the 60%/2000rpm case also experiences an increase in
345 pedal position for the same output torque as the degree of fouling increases. As before, the injector
346 pulse width is increased (figure 8a) however here there is also a change in start of injection with the
347 timing advanced when the injector is fouled. Interestingly the end of main injection appears
348 unchanged. As before, a similar mass of fuel is injected in the clean and fouled conditions, but it is
349 injected over a longer period when fouled. Figure 8b shows the change in main injection over the
350 fouling-clean up cycle and figure 8c shows the resultant change in 50% burn angle.

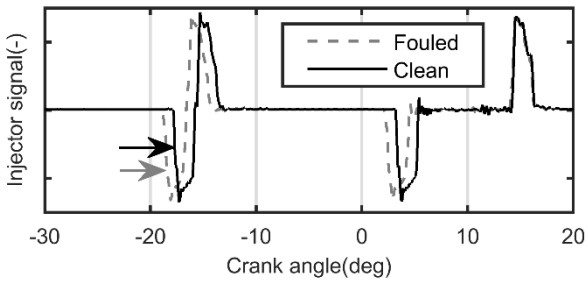

351 (a)

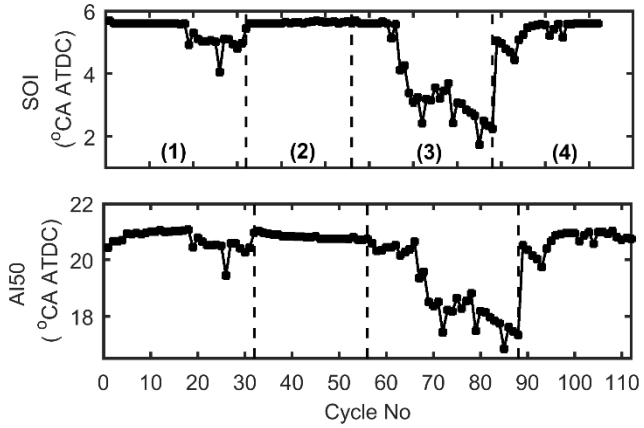

(b)

(1) B7 Dirty-up (2) B7 Clean up

(3) RF79-07 Dirty-up (4) RF79-07 Clean-up

Figure 8: (a) Injector signal at 60% load and 2000rpm for B7 fuel in fouled and clean condition (b) variation in main SOI and (c) 50% burn angle (AI50) combustion over the fouling/Clean-up cycles.

The change in injection timing is interesting at this operating condition as it shows that the engine control strategy is changing as a result of the higher accelerator pedal actuation. Other engine control parameters are affected in a similar way. Figure 9 shows that fuel injection pressure is increased by 3MPa and 7MPa respectively for B7 and reference fuel when fouled. This can be shown to equated to up to 4% increase in injection pump work using equation 8.

$$P_{fuel\ pumping} = \frac{\left(P_{rail} - P_{supply}\right)}{\rho_{fuel}} \dot{m}_{fuel} \qquad \mathbf{8}$$

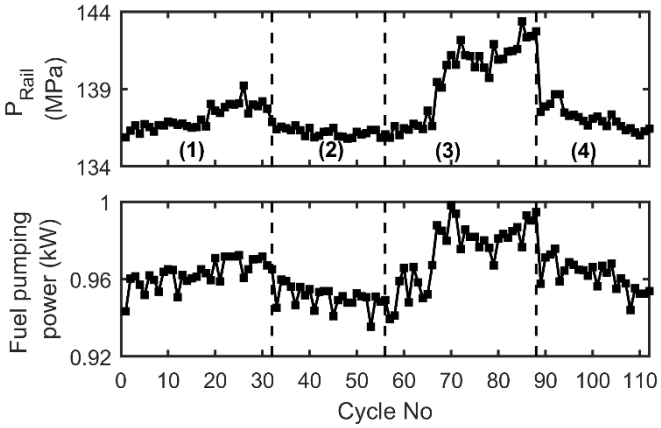

(1) B7 Dirty-up (2) B7 Clean up

(3) RF79-07 Dirty-up (4) RF79-07 Clean-up

Figure 9: Change in (a) fuel rail pressure and (b) fuel pump power over the fouling/clean-up cycles

The increase in pedal position and fuelling demand means that the engine requests a higher air flow through the engine and increases the boost pressure setpoint to achieve this. This results in an increase in VGT angle of up to 4% which in turn increases PMEP by 0.2bar and 0.3bar for B7 and reference fuels respectively when fouled. It is important to note that this is the same underlying mechanism as at the 80% load condition, however at 60% load the effects are more prevalent as the control is more sensitive to the change in pedal position. The mechanism for increased pumping loss at part load is similar to that at full load: there is a lack of exhaust enthalpy compared to the operating point that the engine expects. However, at full load this is due to a lack of fuel mass whereas at part load this is due to an excessive target-load; i.e. at part load the ECU is requesting air mass for a load above the load point at which the engine is actually running.

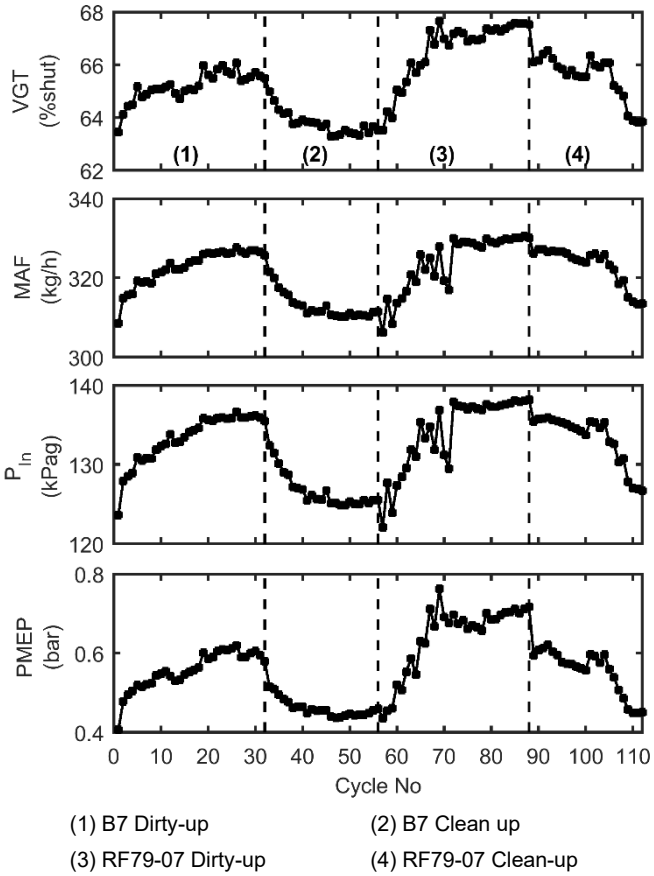

Figure 10 VGT position MAF and PMEP at 60% load

5.3 WLTC Results

5.3.1 Fouling indicators

The WLTC cycles are considered as representative of real world driving in terms of the operating points covered by the engine. The cycles are effectively composed of a sequence of part load operating points and therefore it is expected that some of the factors apparent in the part load points of the CEC cycles will be visible during these tests. Figure 11 shows the profile of key variables throughout the WLTC cycle. The cycle results are commonly treated as four phases representing different speed/load intensity: low, medium, high and extra-high as is shown in Figure 12.

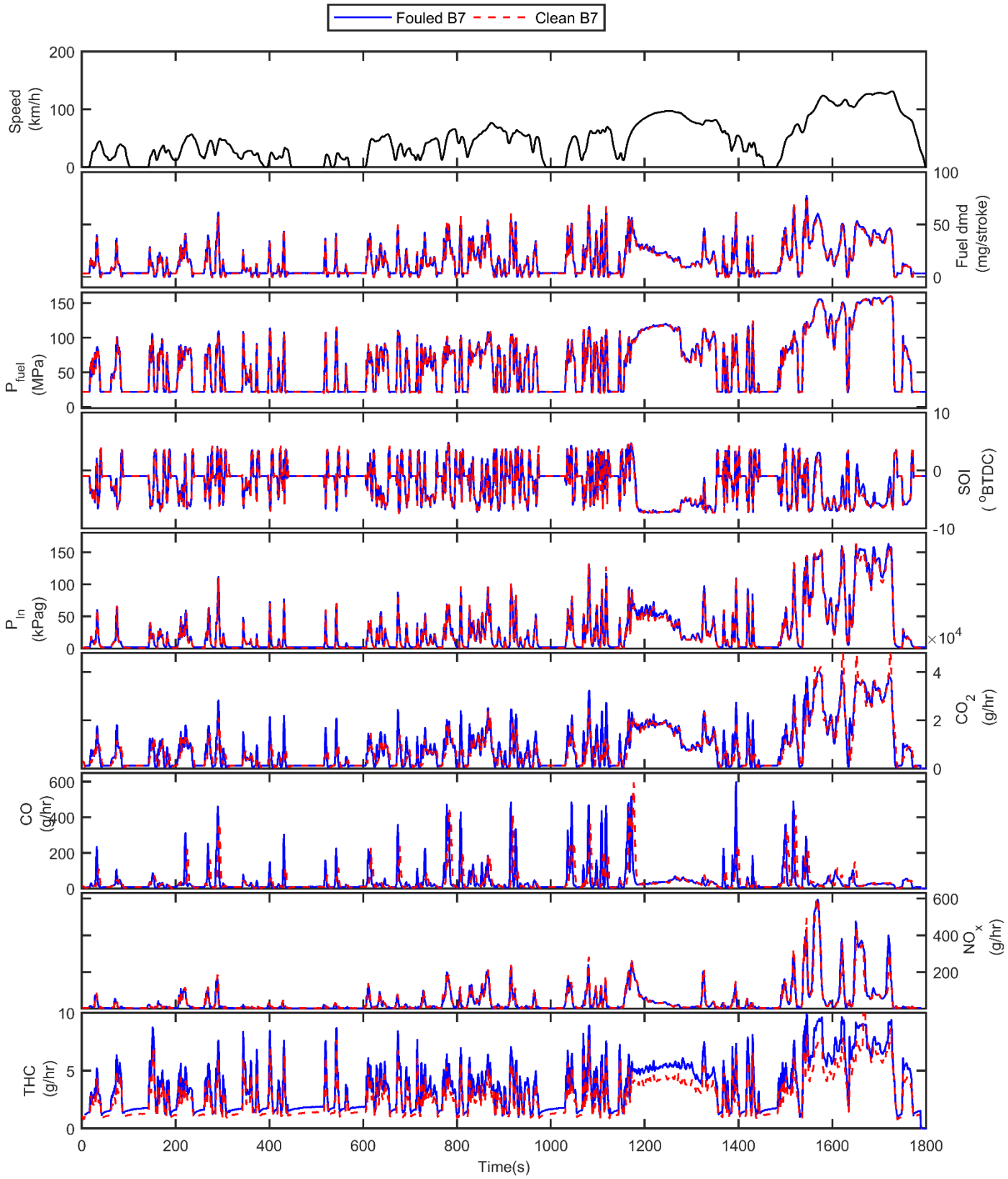

Figure 11: Time based results from the hot start WLTC cycle illustrating simulated vehicle speed, fuelling demand, injection pressure, main injection timing, boost pressure and emissions of CO_2, CO, NOx and THC

Figure 12 shows average pedal position over hot and cold start cycles. These show that the effects of fouling which result in a higher pedal position are visible during all phases of the cycle but that these are more marked in the higher power phases. The pedal position in the low power phase is approximately 3.5% higher when fouled compared to 6% for the extra high phase.

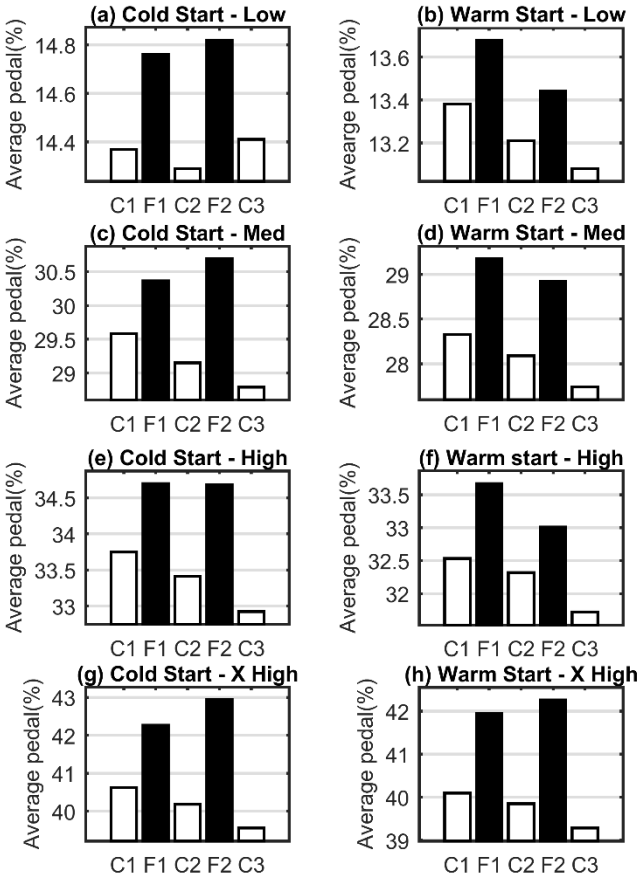

Figure 12: Average pedal position for cold and hot start for the Low (a, b), Medium (c, d) High (e, f) and Extra High (g, h) phases of the WLTC cycle

Figure 13 shows that consistent with the CEC test, over the extra high phase of the WLTC there is an increase in average injection pressure of around 1-2MPa with fouled injectors. At the same time, it was seen that average start of main injection timing was advanced by 0.2-0.5°.

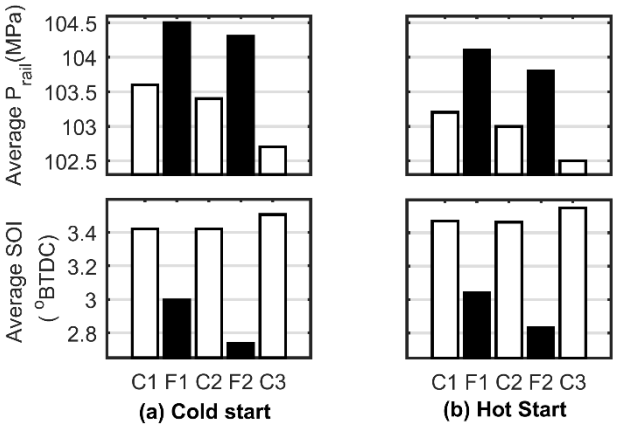

404

405 **Figure 13: Average injection pressure and main SOI over the extra high speed phase of the**
406 **WLTC cycles for (a) cold start and (b) hot start**

407 Figure 14 shows the trends for average VGT position, mass air flow and pumping mean
408 effective pressure (PMEP) over the extra high-speed phase of the WLTC tests. The fouled injectors
409 clearly show an increase in VGT position resulting from the increased boost pressure target caused by
410 the higher pedal position. This in turn results in higher mass air flows and higher PMEP. The average
411 VGT position is increased by 1-1.5% points and the consequent change in average mass air flow is
412 around 5-15kg/h. The increase in PMEP is around 0.05-0.15bar.

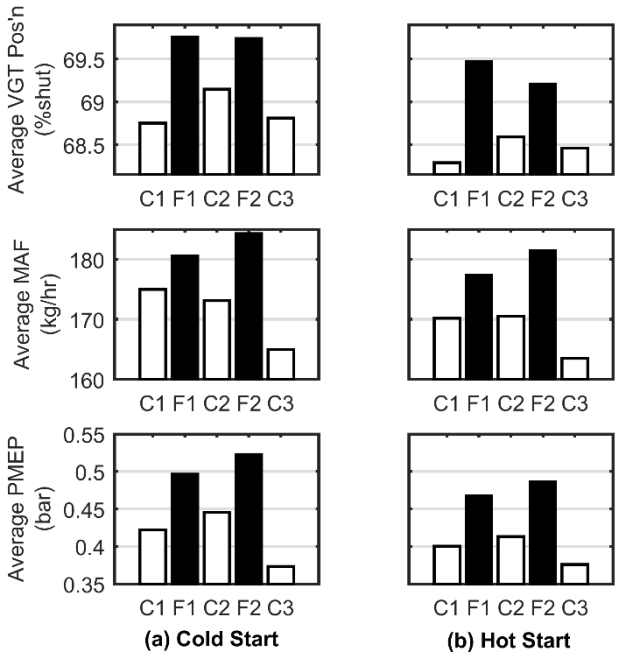

413

414 **Figure 14: Average VGT Position, Mass air Flow and PMEP over the extra high speed phase**
415 **of the WLTC cycle for (a) cold start and (b) hot start**

416 Changes in the amount of exhaust gas recirculation (EGR) were also observed during the WLTC
417 cycles. This was captured through changes in the mean EGR valve position which was seen to be more

closed over the extra high phase of the WLTC (Figure 15a). This is most likely to be a consequence of the change in pedal position caused by the fouled injectors leading to different setpoints for EGR rate in the fouled condition compared to the clean condition. This closed EGR valve clearly correlates with an increase in average mass air flow of 2.5-5% over the extra high phase (Figure 15b). EGR flow was estimated based on conducting an energy balance of flows entering the engine intake manifold and this suggests lower EGR mass flow rates, particularly marked for the second fouled test (Figure 15c) where the EGR mass flow rate is over 15% lower than all clean tests. Finally, NOx emissions are 10% to 20% higher in the fouled WLTC tests which is a strong indicator that EGR rates have been reduced in the fouled injector conditions, particularly in the higher fouling reference fuel test. It should be noted that the emissions changes are effectively 'engine-out' and not 'tailpipe' as no exhaust after-treatment was fitted.

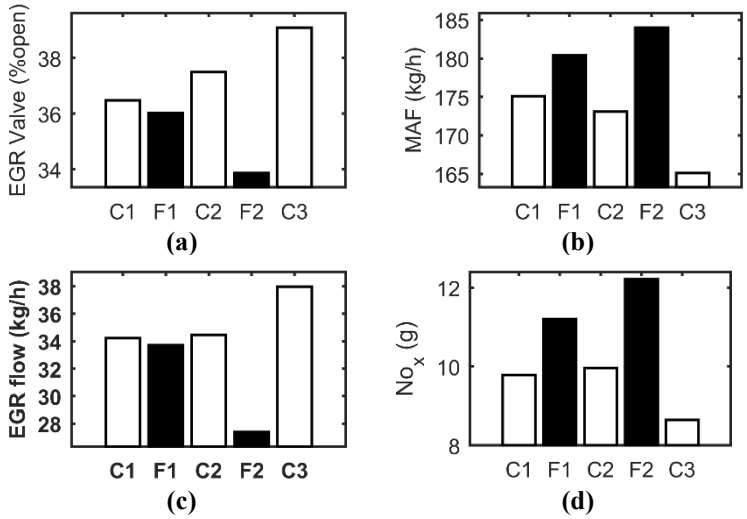

Figure 15: (a) Mean EGR Valve opening, (b) mean mass air flow, (c) mean EGR flow and (d) mean NOx emissions over the extra high phase of the cold start WLTC tests

5.3.2 Emissions and fuel consumption

Figure 16 summarises the overall results from the WLTC cycles for CO_2, NOx, CO and HC emissions and Fuel consumption.

The CO_2 results tend to indicate just over 1% higher total emissions with fouled injectors. However, because the CO_2 analyser failed to sample during the WLTC prior to the first fouling cycles, this is based on two datapoints with the injectors in fouled condition and two with the injectors in clean condition and so it is difficult to conclude that there is a definite trend between fouling and higher CO_2 emissions. Fuel flow can be seen to have a poor correlation with the CO_2 results which reduces the confidence in these results. Furthermore, higher fuel consumption would be expected in the cold start tests due to higher engine frictional losses; a trend that is observed in the CO_2 but absent

from the fuel consumption data. Confidence in the fuel flow measurements is low because although this is a direct measurement, the stability of the measurement can be affected by the repeated fuel flushing process.

Engine out CO and unburnt hydrocarbon emissions during the warm and cold start WLTCs tend to indicate no obvious effect in line with fouling, except in the case of cold start CO which shows lower CO with fouled injectors. This could be an effect of lower EGR rate with fouled injectors.

The total engine-out NOx emissions over the WLTC correlate strongly with the state of the injectors: both fouled conditions show 9% to 18% higher NOx emissions than the clean conditions. The increase in NOx emissions appears to be linked with the change in target-load within the ECU and it has already been shown how this increases the boost pressure target and EGR rates. When this is combined with changes in injection timing and combustion phasing, it is not surprising to see changes in NOx emissions of this magnitude.

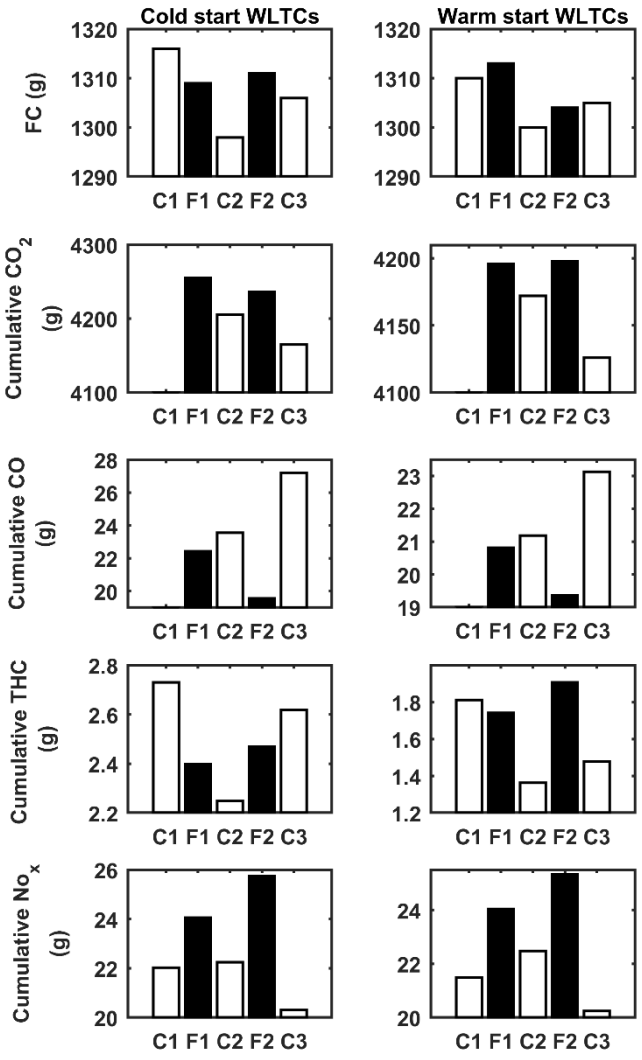

455 **Figure 16: Emissions variations over cold and hot start WLTC cycles**

456

457 6 Discussion

458 A review of the state of the art highlighted the relatively small number of metrics that
459 have been used to quantify or analyse the effects of injector fouling in diesel engines. This
460 demonstrated the scope for undertaking a thorough analysis of the various impacts of injector
461 fouling on Diesel engine behaviour.

462 A drop in peak engine torque of 4% and 8% was demonstrated for B7 and CEC
463 reference fuels respectively over 32h of fouling cycles. This is lower than many published
464 results observed in the CEC F98-08 test standard, however the current study uses standard (not
465 sensitised) injector hardware and a slightly lower duty test cycle (along with higher zinc pro-
466 foulant levels). In this work it is the new metrics describing the impacts of injector fouling
467 which are focussed on and the fact the degree of fouling is lower means that these effects are
468 likely to be even more pronounced and more easily observed in engines that are more
469 susceptible to fouling or have accumulated deposits over longer durations.

470 A new metric for the degree of fouling was introduced as the ratio of output power to
471 fuelling demand. This was devised to account for changes in fuelling demand that the ECU
472 was making in response to lambda variation and which impacted torque. This metric can be
473 used at full load where reduced fuelling occurs and at part load where increased injector pulse
474 width occurs. The following results are quoted for the conditions at which 4% and 8% decreases
475 in peak power occurred, as described above.

476 At full load, a reduction in exhaust gas enthalpy was shown to result in an increase in
477 charge pumping work. When injectors are fouled, the engine controller seeks to maintain boost
478 pressure, but the reduction in fuel flow reduces exhaust temperature by 25°C to 35°C. The
479 controller closes the guide vanes of the variable geometry turbocharger by 2-3% and succeeds
480 in maintaining boost pressure but at the expense of almost doubling PMEP.

481 At part load, fuelling quantity is maintained by increasing the injection duration. This
482 in turn increases the combustion duration – fuel takes longer to burn because it is delivered
483 more slowly into the combustion chamber. At 80% load, the injector pulse width increases by
484 about 12% and AI50 is retarded by up to 1.3°CA, which was modelled to be equivalent to up
485 to 3% worse brake thermal efficiency, (if only AI50 had changed). In practice, the increase in

injector pulse width is achieved by pressing harder on the engine accelerator pedal. This in turn changes the demanded engine torque and a large number of engine control setpoints are altered. At 60% load this was shown to:

1. advance injection timing by up to 3°CA,
2. increase fuel injection pressure by up to 10MPa and fuel pump work by up to 4%.
3. Change the air flow and boost pressure targets which in turn impact on pumping losses.

Over the WLTC drive cycle, the effects seen in the steady state testing at part load were also observed, led by increases in accelerator pedal position when the injectors were fouled. These were most notable during the extra high speed phase of the WLTC. The observed effects were:

1. 0.2-0.5°CA advance in main SOI.
2. 1-2MPa increase in injection pressure.
3. 1-1.5% point increase in VGT position (more closed).
4. 5-15kg/h increase in mass air flow.
5. 0.05-0.15bar increase in PMEP.
6. A decrease in EGR valve opening correlating with up to 15% reduction in EGR mass flow.

Emissions were also measured over the WLTC cycles, these showed trends for just over 1% higher CO_2 emissions with fouled injectors, however this change was not observed in the direct fuel flow measurements which could have been affected by aeration due to switching between fuels. This highlights the difficulty associated with the direct measurement of changes in engine system efficiency as a result of fouled injectors.

During cold start WLTCs, engine-out NOx was substantially higher and CO lower with fouled injectors with both effects thought to be largely due to the reduction in EGR with fouled injectors leading to lower oxygen content in the cylinder and later, cooler combustion. The current air quality debate would suggest that the increase in NOx is of greater significance than the reduction in CO. It is postulated that higher engine-out NOx could also translate to higher AdBlue consumption in vehicles fitted with urea-SCR systems with closed loop control of tailpipe NOx, based on the differences in engine-out NOx observed in this experiment.

The results presented in this work provide new insights into the mechanisms that occur in a LD Euro 5 Diesel propulsion system when injector fouling occurs and when fouling is reversed using premium levels of detergent additives. These factors influence the tertiary effects of injector fouling such as fuel consumption, efficiency and emissions. The findings in this work provide insight to understanding the effects of injector fouling and therefore the benefits of preventing or reversing these effects via the use of premium levels of fuel additives.

Other findings from the study were that the impact of injector fouling can be greatly dependent on the condition at which the engine is operating. This is illustrated by the range of effects on PMEP, rail pressure and emissions at different conditions as discussed above. Fuel type was also found to have a substantial impact on fouling severity. This in turn could mean that real world impacts of injector fouling are different and extend to more parameters than those measured in industry standard tests such as the CEC F98-08 DW10B test.

7 Conclusions

A detailed and extensive experimental investigation was conducted at the University of Bath on a light-duty 2.2L Euro 5 engine to generate new understanding of the impact of diesel injector cleanliness. Some effects of injector fouling were identified for the first time both under steady state conditions and over the World Harmonised Light Duty Cycle, a transient duty cycle representative of on-road conditions. The newly identified effects provide new insights into understanding the consequences of injector fouling and the benefits its prevention will yield. From the work it can be concluded that: -

- At full load conditions with fouled injectors, PMEP can be substantially increased due to the turbocharger working harder to maintain target mass air flow when deposits restrict fuel injection quantity and hence energy in the exhaust gas.
- With fouled injectors, combustion can be retarded at high part-load due to later end of injection which was shown via modelling to be equivalent to up to 3% reduction in brake thermal efficiency relative to clean injectors when all other parameters are kept constant.
- At high part load, fouled injectors lead to incorrect (excessive) fuel injection and charge air pressure due to injector fouling being interpreted by the EMS as a higher load demand, with the latter causing increased PMEP.

- Over the WLTC, similar trends were observed as for the high part load in the CEC cycle, particularly in the high and extra-high sub-cycles of the test.
- In WLTC tests with cold engine starts, engine-out NOx was increased by 9%-18% with fouled injectors, primarily due to the EMS misinterpreting injector fouling as a higher load demand and reducing EGR rate.
- CO_2 increased by 1% with fouled injectors in WLTC tests.
- There is substantial variation in the effects of injector deposits depending on the operating condition with effects tending to be larger at higher loads and differing between WLTC tests run with hot and cold engine starts.
- Different base fuels can lead to different injector fouling propensities.
- The effects of diesel injector nozzle fouling extend beyond the power and flow metrics normally reported in industry tests and can be reversed with premium levels of detergent additives.

8 References

1. Caprotti R, Fowler WJ, Lepperhoff G, Houben M, editors. Diesel additive technology effects on injector hole erosion/corrosion, injector fouling and particulate traps. Fall Fuels and Lubricants Meeting and Exposition, October 18, 1993 - October 21, 1993; 1993; Philadelphia, PA, United states: SAE International, SAE Paper Number 932739, DOI 10.4271/932739
2. Barker J, Richard P, Snape C, Meredith W., 2011. “Diesel Injector Deposits - An Issue That Has Evolved with Engine Technology”, SAE Technical Paper 2011-01-1923, doi:10.4271/2011-01-1923
3. Caprotti R, Breakspear A, Graupner O, Klaua T., 2005. “Detergency Requirements of Future Diesel Injection Systems”, SAE Technical Paper 2005-01-3901, doi:10.4271/2005-01-3901
4. Tang J, Pischinger S, Lamping M, Körfer T, Tatur M, Tomazic D., 2009. “Coking phenomena in nozzle orifices of DI-diesel engines”, SAE Technical Paper 2009-01-0837, doi:10.4271/2009-01-0837
5. Velaers, A., de Goede, S., Woolard, C. and Burnham, R., "Injector Fouling Performance and Solubility of GTL Diesel Dosed with Zinc," SAE Int. J. Fuels Lubr. 6(1):2013, doi:10.4271/2013-01-1697.

6. Xu H, Wang C, Ma X, Sarangi AK, Weall A, Krueger-Venus J. Fuel injector deposits in direct-injection spark-ignition engines. Progress in Energy and Combustion Science. 2015;50:63-80, DOI 10.1016/j.pecs.2015.02.002
7. Henkel S, Hardalupas Y, Taylor A, Conifer C, Cracknell R, Goh TK, et al. Injector Fouling and Its Impact on Engine Emissions and Spray Characteristics in Gasoline Direct Injection Engines. SAE International Journal of Fuels and Lubricants. 2017;10(2), SAE Paper Number 2017-01-0808, DOI 10.4271/2017-01-0808
8. Gueit J, Obiols J, editors. Injector Fouling in Direct Injection Spark Ignition Engines - A New Test Procedure for the Evaluation of Gasoline Additives. SAE 2017 International Powertrains, Fuels and Lubricants Meeting, FFL 2017, October 15, 2017 - October 19, 2017; 2017; Beijing, China: SAE International, SAE Paper Number 2017-01-2294, DOI 10.4271/2017-01-2294
9. Badawy T, Attar MA, Xu H, Ghafourian A. Assessment of gasoline direct injector fouling effects on fuel injection, engine performance and emissions. Applied Energy. 2018;220:351-74, DOI 10.1016/j.apenergy.2018.03.032
10. Zhou J, Pei Y, Peng Z, Zhang Y, Qin J, Wang L, et al. Characteristics of near-nozzle spray development from a fouled GDI injector. Fuel. 2018;219:17-29, DOI 10.1016/j.fuel.2018.01.070
11. Shanahan, C., Smith, S., and Sears, B., "A General Method for Fouling Injectors in Gasoline Direct Injection Vehicles and the Effects of Deposits on Vehicle Performance," SAE Int. J. Fuels Lubr. 10(3):2017, doi:10.4271/2017-01-2298.
12. Jiang C, Xu H, Srivastava D, Ma X, Dearn K, Cracknell R, et al. Effect of fuel injector deposit on spray characteristics, gaseous emissions and particulate matter in a gasoline direct injection engine. Applied Energy. 2017;203:390-402, DOI 10.1016/j.apenergy.2017.06.020
13. Magno A, Mancaruso E, Vaglieco BM. Experimental investigation in an optically accessible diesel engine of a fouled piezoelectric injector. Energy. 2014;64:842-52, DOI 10.1016/j.energy.2013.10.071
14. Risberg PA, Alfredsson S. The Effect of Zinc and Other Metal Carboxylates on Nozzle Fouling. SAE International; 2016, SAE Paper Number 2016-01-0837, DOI 10.4271/2016-01-0837
15. Barbour RH, Quigley R, Panesar A, editors. Investigations into Fuel Additive Induced Power Gain in the CEC F-98-08 DW10B Injector Fouling Engine Test. SAE 2014 International Powertrains, Fuels and Lubricants Meeting, FFL 2014, October 20, 2014 - October 22, 2014; 2014; Birmingham, United kingdom: SAE International, SAE Paper Number 2014-01-2721, DOI 10.4271/2014-01-2721

16. Barker J, Langley GJ, Richards P, editors. Insights into deposit formation in high pressure diesel fuel injection equipment2010: SAE International, SAE Paper Number 2010-01-2243, DOI 10.4271/2010-01-2243
17. Williams RG, Balthasar, F; Diesel Fuel Degradation and Contamination in Vehicle Systems. 2009 TAE Esslingen Fuels Conference
18. Hawthorne M, Roos JW, Openshaw MJ, editors. Use of fuel additives to maintain modern diesel engine performance with severe test conditions. 2008 SAE International Powertrains, Fuels and Lubricants Congress, June 23, 2008 - June 25, 2008; 2008; Shanghai, China: SAE International, SAE Paper Number 2008-01-1806, DOI 10.4271/2008-01-1806
19. Zampilli M, Bartocci P, Bidini G, Fantozzi F, editors. A Quantitative Methodology to Measure Injector Fouling Through Image Analysis. 71st Conference of the Italian Thermal Machines Engineering Association, ATI 2016, September 14, 2016 - September 16, 2016; 2016; Torino, Italy: Elsevier Ltd, DOI 10.1016/j.egypro.2016.11.088
20. D'Amico M, Zampilli M, Laranci P, D'Alessandro B, Bidini G, Fantozzi F, editors. Measuring injectors fouling in internal combustion engines through imaging. 70th Conference of the Italian Thermal Machines Engineering Association, ATI 2015, September 9, 2015 - September 11, 2015; 2015; Rome, Italy: Elsevier Ltd, DOI 10.1016/j.egypro.2015.11.873
21. Miura Y, Miyahara K, Sasaki S, Kashio T, Yoshida K, editors. Development of a Gasoline Direct Injector Fouling Test and Its Application to Study of Keep-Clean Performance at Different Additive Treat Rates. SAE International Powertrains, Fuels and Lubricants Meeting, FFL 2016, October 24, 2016 - October 26, 2016; 2016; Baltimore, MD, United states: SAE International, SAE Paper Number 2016-01-2248, DOI 10.4271/2016-01-2248
22. de Goede, S., Barbour, R., Velaers, A., Sword, B. et al., "The Effect of Near-Zero Aromatic Fuels on Internal Diesel Injector Deposit Test Methods," SAE Int. J. Fuels Lubr. 10(1):2017, doi:10.4271/2017-01-0807.
23. De Goede S, Roets P, Velaers A, Vermeulen J, Wilken C, editors. The properties and injector nozzle fouling performance of GTL and EN590 diesel with RME and SME biodiesel. SAE 2013 World Congress and Exhibition, April 16, 2013 - April 18, 2013; 2013; Detroit, MI, United states: SAE International, SAE Paper Number 2013-01-1136, DOI 10.4271/2013-01-1136
24. Richardson CB, Gyorog DA, Beard LK, editors. A laboratory test for fuel injector deposit studies. International Fuels and Lubricants Meeting and Exposition, September 25, 1989 - September 28, 1989; 1989; Baltimore, MD, United states: SAE International, SAE Paper Number 892116, DOI 10.4271/892116

25. D'Ambrosio S, Ferrari A. Diesel injector coking: Optical-chemical analysis of deposits and influence on injected flow-rate, fuel spray and engine performance. Journal of Engineering for Gas Turbines and Power. 2012;134(6), DOI 10.1115/1.4005991
26. Smith, A. and Williams, R., "Linking the Physical Manifestation and Performance Effects of Injector Nozzle Deposits in Modern Diesel Engines," SAE Int. J. Fuels Lubr. 8(2):2015, doi:10.4271/2015-01-0892.
27. Arpaia A, Catania AE, D'Ambrosio S, Ferrari A, Luisi SP, Spessa E, editors. Injector coking effects on engine performance and emissions. 2009 ASME Internal Combustion Engine Division Fall Technical Conference, ICEF 2009, September 27, 2009 - September 30, 2009; 2009; Lucerne, Switzerland: American Society of Mechanical Engineers (ASME), DOI 10.1115/ICEF2009-14094
28. Kumagai S, Takahashi A, Nagato H, Stradling RJ, editors. Development of an Injector Deposit Formation Test Method for a Medium-Duty Diesel Engine. JSAE/SAE 2015 International Powertrains, Fuels and Lubricants Meeting, FFL 2015, September 1, 2015 - September 4, 2015; 2015; Kyoto, Japan: SAE International, SAE Paper Number 2015-01-1914, DOI 10.4271/2015-01-1914
29. Williams R, Development of a nozzle fouling test for additive rating in heavy duty di diesel engines. Powertrain and Fluid Systems Conference and Exhibition, October 21, 2002 - October 24, 2002; 2002; San Diego, CA, United states: SAE International, SAE Paper Number 2002-01-2721, DOI 10.4271/2002-01-2721
30. Barbour R, Arters D, Dietz J, MacDuff M, Panesar A, Quigley R, editors. Diesel detergent additive responses in modern, high-speed, direct-injection, light-duty engines. JSAE/SAE International Fuels and Lubricants Meeting, JSAE 2007, July 23, 2007 - July 23, 2007; 2007; Kyoto, Japan: SAE International, SAE Paper Number 2007-01-2001, DOI 10.4271/2007-01-2001
31. Magno A, Mancaruso E, Vaglieco BM, Florio S, Gioco G, Rebesco E, editors. Study on spray injection and combustion of fouled and cleaned injectors by means of 2-D digital imaging in a transparent CR diesel engine. 11th International Conference on Engines and Vehicles, ICE 2013, September 15, 2013 - September 19, 2013; 2013; Capri, Naples, Italy: SAE International, SAE Paper number 2013-24-0062, DOI 10.4271/2013-24-0062
32. Richards P, Walker RD, Williams D, editors. Fouling of two stage injectors - An investigation into some causes and effects. International Spring Fuels and Lubricants Meeting, May 5, 1997 - May 8, 1997; 1997; Dearborn, MI, United states: SAE International, SAE Paper number 971619, DOI 10.4271/971619
33. Pos R, Cracknell R, Ganippa L. Transient characteristics of diesel sprays from a deposit rich injector. Fuel. 2015;153:183-91. DOI10.1016/j.fuel.2015.02.114

34. Behrendt, C. and Smith, A., "A Study of Diesel Fuel Injector Deposit Effects on Power and Fuel Economy Performance," SAE Technical Paper 2017-01-0803, 2017, https://doi.org/10.4271/2017-01-0803
35. Dowell PG, Akehurst S, Burke RD. Accuracy of Diesel Engine Combustion Metrics over the Full Range of Engine Operating Conditions. Journal of Engineering for Gas Turbines and Power. 2019;141(9), DOI: 10.1115/1.4043700
36. Hohenberg, G.F., Advanced Approaches for Heat Transfer Calculations, SAE Paper No. 790825, 1979, DOI: https://doi.org/10.4271/790825
37. UN GTR No. 15 - Worldwide harmonized Light Vehicles Test Procedure (ECE/TRANS/180/Add.15), 12th March 2014, available from: https://www.unece.org/trans/main/wp29/wp29wgs/wp29gen/wp29glob_registry.html, accessed 01/08/2017.
38. Bielaczyc, P., Woodburn, J., and Szczotka, A.A., "Comparison of Carbon Dioxide Exhaust Emissions and Fuel Consumption for Vehicles Tested over the NEDC, FTP-75 and WLTC Chassis Dynamometer Test Cycles," SAE Technical Paper 2015-01-1065, 2015, doi:10.4271/2015-01-1065.
39. Dowell P, Akehurst S, Burke R. An improved rate of heat release model for modern high speed diesel engines. Journal of Engineering for Gas Turbines and Power: Transactions of the ASME. 2017 Sep 1;139(9). 092805. https://doi.org/10.1115/1.4036101

9 Appendix

The Characteristics of the vehicle are provided in table 6. The engine speed and load were calculated according to equations 9 and 10 where the load and inertia are dependent on the selected gear ratio. Equation 9 provides the relationship between vehicle speed and ending speed whilst equation 10 describes the engine torque which is composed of the vehicle load and the inertia force. The inertia is calculated by reflecting the inertias of the driveline and the mass of the vehicle back to the engine crankshaft.

$$\omega_{eng} = \frac{V_{veh}}{2\pi r_w} GR \qquad \mathbf{9}$$

$$\tau_{eng} = \dot{\omega}_{eng} I_{veh} + \tau_{drag} \qquad \mathbf{10}$$

Where

$$I_{veh} = \left[I_{prop} + (I_{axle} + (m \times r_w^2) \times R_{FD}^2)\right] \times GR^2$$

$$\tau_{drag} = \frac{\left(\frac{1}{2}\rho_{air} c_d \, A \, {v_{veh}}^2 + mgC_{rr}\right) \times r_w}{R_{FD} \times GR}$$

703

704 The gear shifting strategy was calculated according to the WLTP legislation standards [37, 38].

705 The resultant engine speed and load are shown in figure 17.

706 **Table 6: Vehicle parameters used for WLTC duty cycle**

Parameter	Value
Vehicle Mass	2000kg
Drag Coefficient	0.4
Frontal Area	2.86m^2
Tyre type	265/65R17
Rolling resistance coefficient	0.015
Gear Ratios: 1st gear 2nd gear 3rd gear 4th gear 5th gear 6th gear Final drive	 5.44 2.84 1.72 1.22 1 0.79 3.31
Driveline inertias Prop shaft Axle, wheel and tyres	 0.02kgm^2 2.4kgm^2

707

708

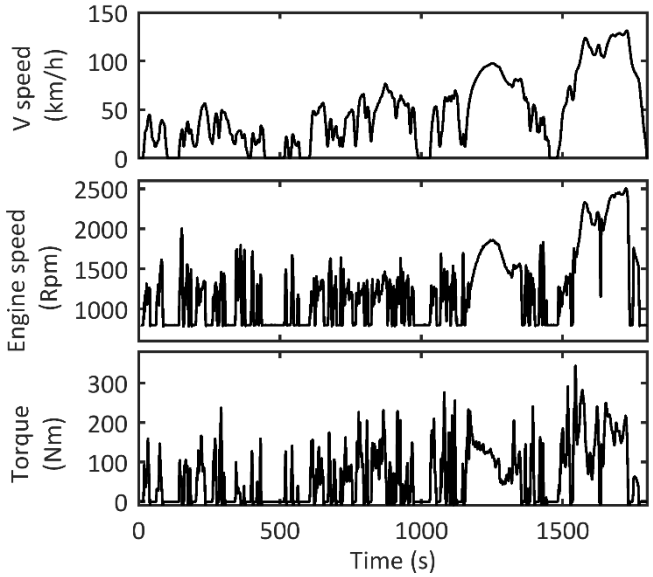

709

710 **Figure 17: WLTC vehicle speed and calculated engine speed and torque**

711